Supporting Information:

Conjugated Polyions Enable Organic Photovoltaics Processed from Green Solvents

Gang Ye,[†,‡] Nutifafa Y. Doumon,[‡] Sylvia Rousseva,[†,‡] Yuru Liu,[†,‡] Mustapha Abdu-Aguye,[‡] Maria A. Loi,[‡] Jan C. Hummelen,[†,‡] L. Jan Anton Koster,[‡] and Ryan C. Chiechi*[,†,‡]

†*Stratingh Institute for Chemistry, University of Groningen, Nijenborgh 4, 9747 AG Groningen, The Netherlands*

‡*Zernike Institute for Advanced Materials, Nijenborgh 4, 9747 AG Groningen, The Netherlands*

E-mail: r.c.chiechi@rug.nl

Contents

1 Synthesis **S-3**

1.1 General S-3

1.2 Monomers S-4

1.3 Polymers S-6

2 Characterization **S-9**

2.1 NMR S-9

2.2 FT-IR S-12

2.3 Thermal properties S-13

2.4 UV-Vis S-15

2.5 Photoluminescence S-16

2.6 Film Morphology S-18

2.7 EQE data of bi-layer solar cells S-19

3 DFT calculations **S-19**

4 SCLC measurement **S-20**

5 Impedance device **S-21**

6 Impedance data **S-21**

References **S-22**

1 Synthesis

1.1 General

All reagents and solvents were commercial and were used without further purification unless otherwise indicated.

Measurement and characterization. ^{1}HNMR and ^{13}CNMR were performed on a Varian Unity Plus (400 MHz) instrument at 25 °C, using tetramethylsilane (TMS) as an internal standard. NMR shifts are reported in ppm, relative to the residual protonated solvent signals of $CDCl_3$ (δ = 7.26 ppm) or DMSO – d_6 (δ = 2.50 ppm) and at the carbon absorption in $CDCl_3$ (δ = 77.23 ppm) or DMSO – d_6 (δ = 39.52 ppm). Multiplicities are denoted as: singlet (s), doublet (d), triplet (t) and multiplet (m). High Resolution Mass Spectroscopy (HRMS) was performed on a JEOL JMS 600 spectrometer. FT-IR spectra were recorded on a Nicolet Nexus FT-IR fitted with a Thermo Scientific Smart iTR sampler. Thermal properties of the polymers were determined on a TA Instruments DSC Q20 and a TGA Q50. DSC measurements were executed with two heating-cooling cycles with a scan rate of 10 °C/min, and from each scan, the second heating cycle was selected. TGA measurements were done from 20 °C to 800 °C with a heating rate of 20 °C/min under N_2 flow. EPR spectra were recorded on a Magnettech MiniScope MS400 using a quartz capillary at a concentration of 5-10 mg mL^{-1} in HCOOH. UV-vis-NIR measurements were carried out on a Shimadzu UV 3600 spectrometer in 1 cm fused quartz cuvettes with concentrations of 0.01 mg mL^{-1}. Photoluminescence measurements were carried out on solutions contained in quartz cuvettes. The samples were excited by the second harmonic (approximately 400 nm) of a mode-locked Mira 900 Ti:Sapphire laser delivering 150 ps pulses at a repetition rate of 76 MHz. The laser power was adjusted using neutral density filters; and the excitation beam was spatially limited by an iris. The beam was focused with a 150 mm focal length in reflection geometry. Steady state spectra were collected by a spectrometer with a 50 lines/mm grating and recorded with a Hamamatsu em-CCD array. For time resolved measurements, the same

pulsed excitation source was used. Spectra were in this case collected on a Hamamatsu streak camera working in Synchroscan mode (time resolution ~2 ps) with a cathode sensitive in the visible. All plotted spectra were corrected for the spectral response of the setup using a calibrated lamp. Cyclic voltammetry (CV) was carried out with a Autolab PGSTAT100 potentiostat in a three-electrode configuration where the working electrode was platinum electrode, the counter electrode was a platinum wire, and the pseudo-reference was an Ag wire that was calibrated against ferrocene (Fc/Fc^{+}).

1.2 Monomers

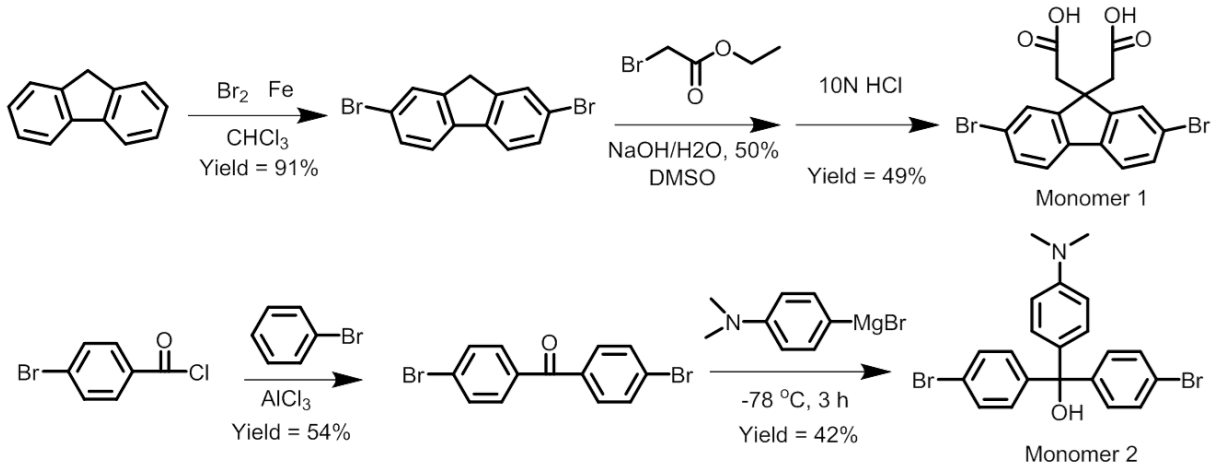

Figure S1: Synthetic route for monomers.

2,7-Dibromo-9H-fluorene

Bromine (63 g, 392 mmol, 20.2 mL) in 40 mL of chloroform was added drop-wise into a suspension solution containing fluorene (30.0 g, 180 mmol), iron powder (160 mg, 2.86 mmol) in a catalytic amount and 200 mL of chloroform. The flask was cooled in ice water, and the temperature was controlled under 5 °C. This is anexothermic reaction, and any rapid addition of the bromine should be avoided. After completion adding bromine, the reaction was allowed to warm to room temperature and stirred overnight at room temperature in darkness. After quenching with saturated aqueous $Na_2S_2O_3$, the product was filtered and

recrystallized from chloroform, to afford white solid (52.5g, 91% yield). ^{1}HNMR (400 MHz, $CDCl_3$): δ: 7.66 (s, 2H), 7.60 (d, J = 8.1 Hz, 2H), 7.50 (d, J = 8.1 Hz, 2H), 3.86 (s, 2H).

Monomer (1), 2,2'-(2,7-dibromo-9H-fluorene-9,9-diyl)diacetic acid [S1]

Ethyl bromoacetate (10.2 g, 60 mmol) was diluted with DMSO (25 mL) and added drop-wise to a solution of 2,7-dibromofluorene (6.44 g, 20 mmol) and sodium hydroxide (50% w/w) aqueous solution (15 mL) in DMSO (150 mL) under nitrogen at 0 °C. After completion addition, the resulting solution was allowed to warm to room temperature and stirred for overnight at room temperature. Then 10N HCl (34 mmol) was added drop-wise to the reaction mixture in ice-water bath. The resulting mixture was kept stirring for 30 min to form precipitate. then precipitate was collected by filtration, followed by washing with water for three times, then the crude product was dissolved into 1N NaOH. the aqueous solution was acidified by addition 1N HCl. A precipitate was collected by filtration and dried in vacuum at 50 °C overnight and was recrystallized from ethanol and CH_2Cl_2 mixture to give white solid product (4.3 g, 49%). ^{1}HNMR (400 MHz, DMSO – d_6): δ : 11.89 (s, 2H, COOH), 7.85(d, 2H, J = 1.8 Hz, Ar-H), 7.78 (d, 2H, J = 8.1 Hz, Ar-H), 7.52 (dd, 2H, J = 8.1 Hz, 1.7 Hz, Ar-H), 3.08 (s, 4H, CH2). ^{13}CNMR (100 MHz, DMSO – d_6) δ: 170.93, 151.36, 138.64, 130.32, 126.71, 122.02, 120.46, 56.03, 41.73.

bis(4-bromophenyl)methanone[S2]

To a nitrogen-purged 3-neck flask containing a solution of 4-bromobenzoyl chloride (4.4 g, 20 mmol) in 20 mL bromobenzene, $AlCl_3$ (5.48 g, 40 mmol) was added at 0 °C. The resulting mixture was allowed to warm to room temperature and stirred overnight, then heated at 90 °C for 3 h, cooled to room temperature. The mixture was quenched by pouring it over 1 N HCl/ice and extracted with CH_2Cl_2, the combined organic layers were washed with water and brine, and dried over Na_2SO_4. The solvents were removed by rotary evaporation. Finally the crude product was recrystallized from MeOH to give a colorless crystal product (3.67 g, 54%). ^{1}HNMR (400 MHz, $CDCl_3$): δ: 7.64 (s, Ar-H, 8H).

Monomer (2), bis(4-bromophenyl)(4-(dimethylamino)phenyl)methanol[S3]

To a solution of bis(4-bromophenyl)methanone (182 mg, 1 mmol) in 10 mL anhydrous THF under an atmosphere of N_2, Gringard reagent (4-(dimethylamino)phenyl)magnesium bromide (0.45 M, 2 mL, 0.9 mmol) was added drop-wise at −78 °C. The solution was stirred for 3 h in the cold bath. Saturated ammonium chloride aqueous solution was added to quench the reaction, and extracted with CH_2Cl_2. The organic phase was dried over Na_2SO_4 and the solvents removed by rotary evaporation. The crude solid was purified by column chromatography to give product (190 mg, 42%). ^{1}HNMR (400 MHz, $CDCl_3$): δ: 7.46 (d, J = 8.6 Hz, 4H), 7.21 (d, J = 8.6 Hz, 4H), 7.03 (d, J = 8.9 Hz, 2H), 6.67 (d, J = 8.9 Hz, 2H), 3.01 (s, OH, 1H), 2.95 (s, N – CH_3, 6H). ^{13}CNMR (100 MHz, $CDCl_3$): δ: 149.98, 146.23, 133.59, 130.87, 129.64, 128.67, 121.10, 111.77, 81.06, 40.25.

1.3 Polymers

The polymers were synthesized by palladium-catalysted Suzuki coupling polymerization of dibromo-monomers with diboronic acid-monomers in a DMF/H_2O solvent mixture. Polymers were obtained under refluxing the polymerization mixture three days. Impurities and low-molecular-weight fraction were removed by dialysis in water. The molecular weight cut off of the dialysis membrane is 3500. After the dialysis, **CPIZ-B** become the red colour due to a little bit carbocation formed during the ionic exchange, while **CPIZ-T** remain yellow colour. After drying under vacuum, our target polymers product was obtained in precursor state. Their chemical structures were characterized by nuclear magnetic resonance (NMR) and fourier-transform infrared (FT-IR) (Figures S2-S5). For the NMR measurement, the data were collected in CF_3COOD due to both polymers show good solubility in organic acids. The proton ratio of aromatic region and aliphatic region is 42:16 for **CPIZ-B** and 36:16 for **CPIZ-T**, respectively. In the acid condition, both **CPIZ-B** and **CPIZ-T** showed ionic state. However, it is hard to check ^{1}HNMR of the polymers as prepared state due to poor solubility in common deuterated solvent such as $CDCl_3$ and DMSO – d_6. FT-IR spectra were carried out to check the chemical structure of the polymers changing from as

prepared state to the protonation state. As shown in the Figrue S5, both polymers have no typical carboxylic acid C=O stretching mode around 1700 cm^{-1} in as prepared state, indicate the carboxylic acid were coordinated with the sodium salt.[S1] This also was confirmed in our model conjugated polyelectrolyte P1. After protonation, the peak around 1700 cm^{-1} enhanced, which indicates that carboxylic acid was dissociated with sodium by the protonation and peak around 1185 cm^{-1} which belongs to the C-O-C stretching mode enhanced,[S4] indicating that there exist the Coulomb interaction between the anion in the side and cation in the backbone. Thus, both appeared and enhanced peaks in IR spectra after treating with acid, suggested both polymers exhibited polyzwitterions in solid state after protonation.

It is not easy to determine the isoelectric points of our CPIs. There are two equilibrium reaction in these compound, first one is the dehydration-hydration reaction, the other is the base-acid reaction. When we turn the pH of CPIs solution, the dehydration-hydration reaction may happen. This disturb the isoelectric points measurement.

General synthetic procedures for polymer

To a dry three-neck flask, Monomer 1 (1 eq), Monomer 2 (2 eq) and Diboronic acid derivatives (3 eq) were added under N_2 followed by Tetrakis(triphenylphosphine)palladium(0) $Pd(PPh_3)_4$ (30 mg). The flask and its contents were subjected to 3 pump/purge cycles with N_2 followed by addition of oxygen-free aqueous solution of 2M Na_2CO_3 (5 mL) and anhydrous, oxygen-free DMF (10 mL) via syringe. The reaction mixture was vigorously stirred at 95 °C for three days. After cooling to room temperature, the reaction mixture was poured into 200 mL vigorously stirred acetone. The precipitated solid was collected by filtration. The solid polymers were suspended in milipore water, and transferred into a dialysis tube (MWCO:3500). The dialysis tube was placed in a large beaker with water (2 L) stirring for 3 days, and the water was changed every 12 hours. After the dialysis, the solid was collected and dried under vacuum overnight.

CPIZ-B: Synthesis according to the general polymerization procedure: monomer 1 (110 mg, 0.25 mmol), monomer 2 (230 mg, 0.5 mmol) and 1,4-phenylenediboronic acid (125 mg, 0.75 mmol).

The polymer was obtained as a red solid (240 mg, 88 %).

^{1}HNMR (400 MHz, TFA – d): δ: 8.6−6.7 (m, Ar-H, 42H), 4.4−2.5 (m, N – CH_3 + CH_2, 16H).

^{1}HNMR (400 MHz, D_2SO_4+DMSO−d_6): δ: 8.25−7.05 (m, Ar-H, 42H), 3.56−2.40 (br, CH_2, 4H), 3.26−2.98 (m, N−CH_3, 12H).

IR (cm^{-1}): 695, 745, 810, 907, 947, 1003, 1153, 1188, 1351, 1396, 1463, 1487, 1518, 1608, 3027.

CPIZ-T: Synthesis according to the general polymerization procedure: monomer 1 (110 mg, 0.25 mmol), monomer 2 (230 mg, 0.5 mmol) and thiophene-2,5-diyldiboronic acid (130 mg, 0.75 mmol). The polymer was obtained as a yellow solid (50 mg, 17%). ^{1}HNMR (400 MHz, TFA−d): δ: 8.4−6.7 (m, Ar-H, 36H), 4.5−2.7 (m, N−CH_3 + CH_2, 16H).

IR (cm^{-1}): 695, 741, 759, 798, 905, 946, 973, 1016, 1153, 1187, 1350, 1405, 1443, 1495, 1518, 1563, 1607, 3356.

2 Characterization

2.1 NMR

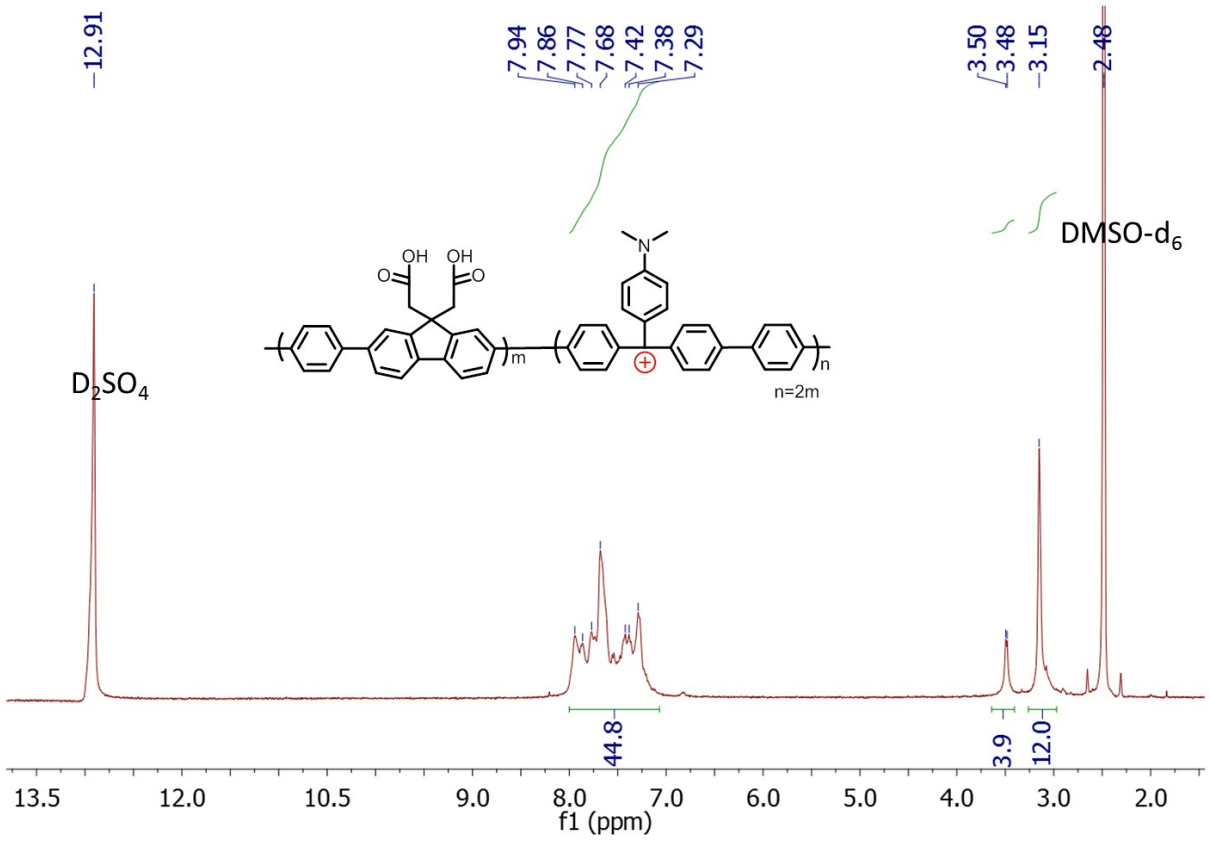

Figure S2: HNMR spectrum of CPIZ-B in D_2SO_4 and DMSO – d_6.

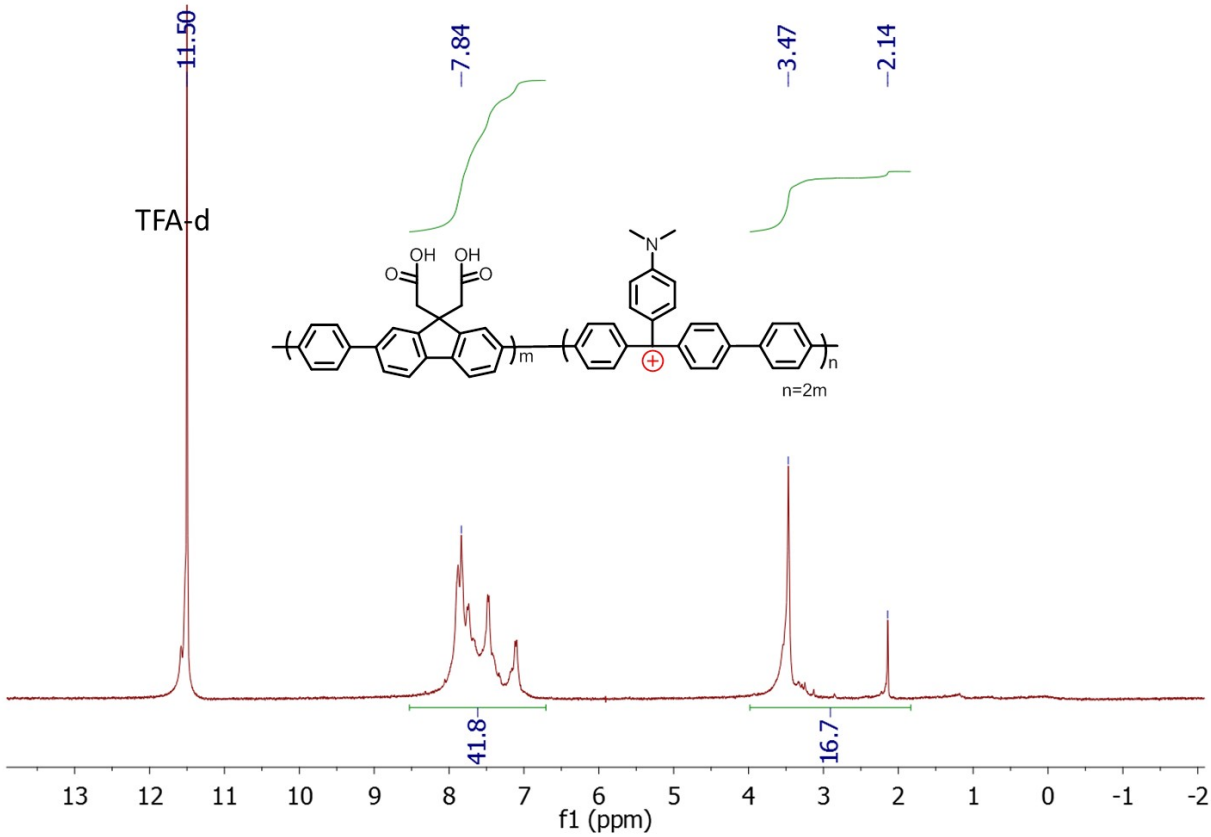

Figure S3: HNMR spectrum of CPIZ-B in TFA –d.

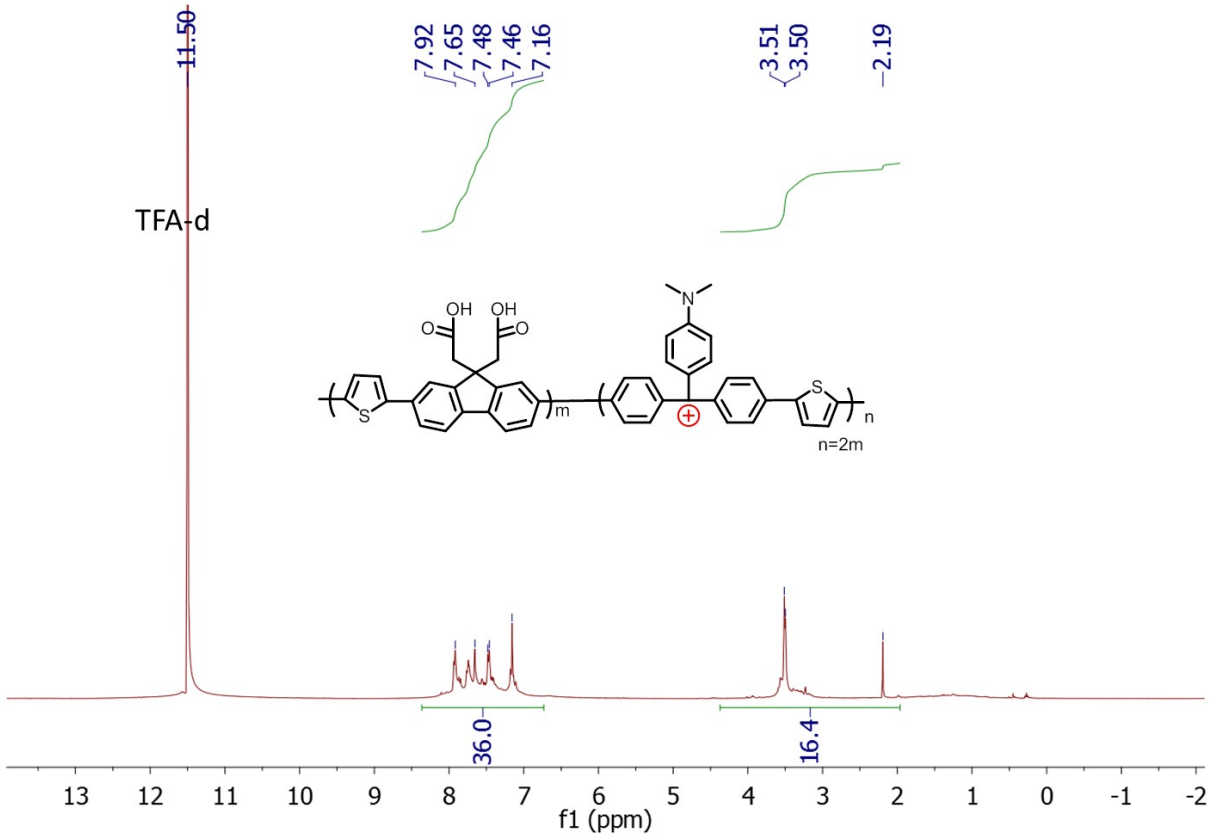

Figure S4: HNMR spectrum of CPIZ-T in TFA – d.

2.2 FT-IR

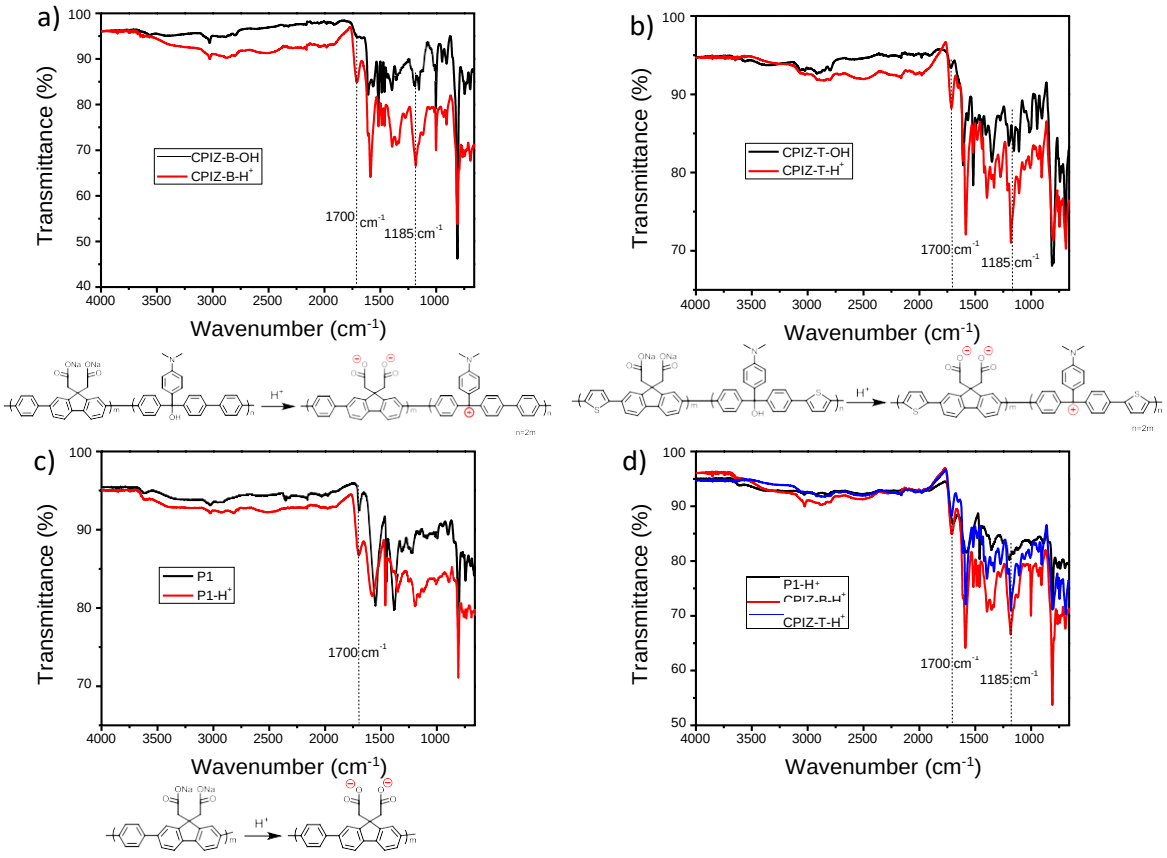

Figure S5: FT-IR spectra of showing a) **CPIZ-B**, b) **CPIZ-T** and c) model polymers P1 before and after treating with HCOOH. d) IR spectra for **CPIZ-B**, **CPIZ-T** and P1 after treating with acid. Both appeared peaks in 1700 cm^{-1} and enhanced peaks in 1185 cm^{-1} spectra after treating with acid, suggested both polymers exhibited polyzwitterions in solid state after protonation.

2.3 Thermal properties

The thermal properties of **CPIZ-B** and **CPIZ-T** in precursor state and in ionic state were investigated by thermogravimetric analysis (TGA) and differential scanning calorimetry (DSC). The TGA results are shown in Figure S6. The temperature of 5% weight-loss was selected as the onset point of thermal degradation temperatures (T_d). Both polymers in precursor and ionic state exhibit similar T_d. **CPIZ-T** even have similar trace, but **CPIZ-B** backbone structure seem became more stable after treating with acid. The good stability with (T_d) at 200 ˚C for **CPIZ-B** and 182 ˚C for **CPIZ-T**, respectively, indicating that they are sufficient thermally stable for devices applications. As shown in Figure S7, the DSC curves of **CPIZ-B** and **CPIZ-T** in both precursor and ionic state show that there are no distinct exothermal transition in the second heating cycle and cooling cycle, revealing that no crystalline behavior or phase transition occurred during this temperature section.

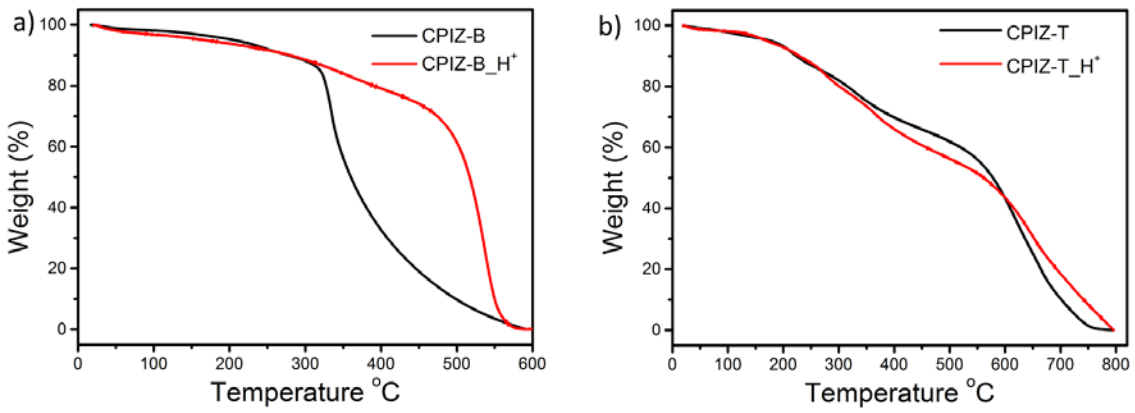

Figure S6: Thermogravimetric analysis plots for **CPIZ-B** a) and **CPIZ-T** b) before and after treating with acid.

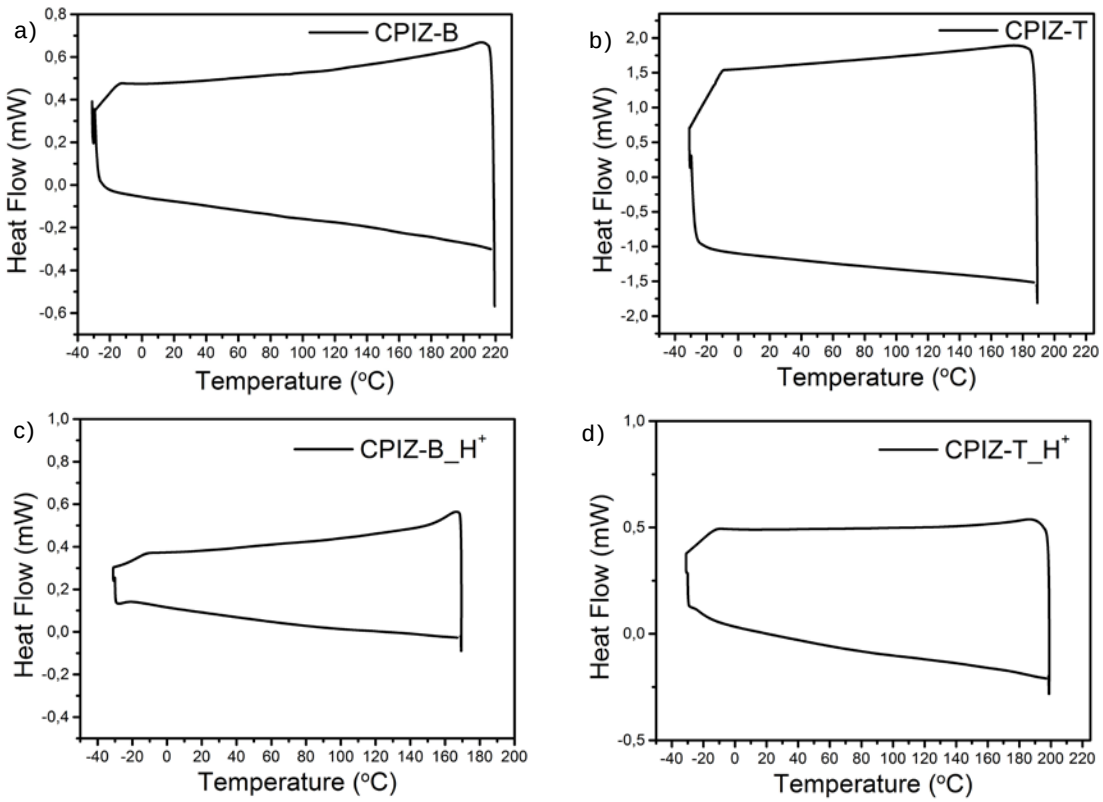

Figure S7: Differential scanning calorimetry curves for **CPIZ-B** a) and **CPIZ-T** b). The measurements were executed with two heating-cooling cycles with a scan rate of 10 °C min^{-1}, and the second heating cycle was selected.

2.4 UV-Vis

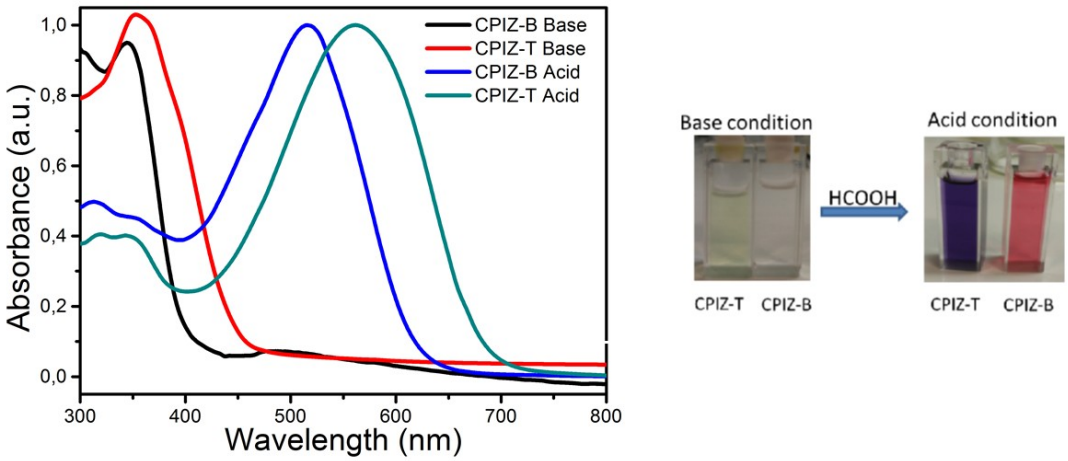

Figure S8: Absorption spectra of conjugated polyions in basic and acidic conditions and the solution colour of conjugated polyions in base water and in pure HCOOH.

2.5 Photoluminescence

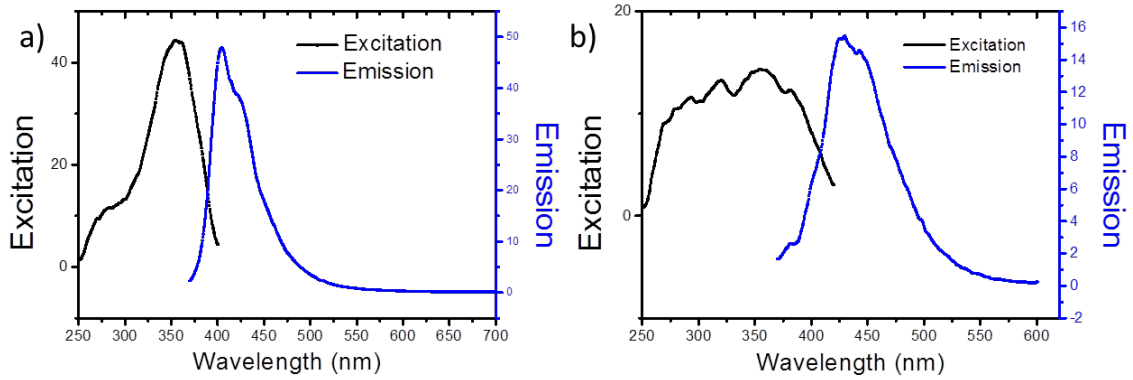

Figure S9: Emission and excitation spectra for **CPIZ-B** a) and **CPIZ-T** b) in HCCOH solution.

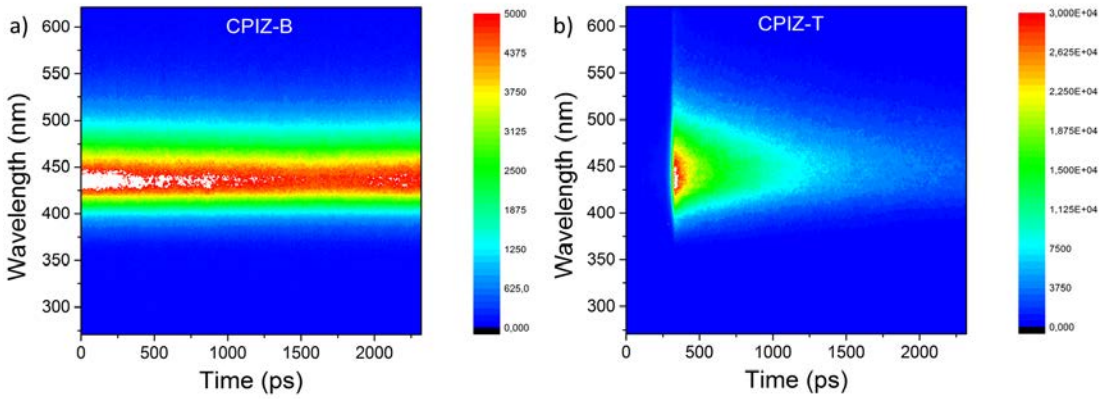

Figure S10: The time-resolved photoluminescence spectra for **CPIZ-B** a) and **CPIZ-T** b) in HCCOH solution. **CPIZ-B** showed longer life time which decay lifetime exceeding 2000 ps which was the maximum measurable lifetime of the streak camera unit, while **CPIZ-T** showed bimodal-exponential photoluminescence decay with lifetimes of 146 ps and 969 ps.

Figure S9 show the steady-state fluorescence spectra of **CPIZ-B** and **CPIZ-T**, and their excitation spectra in HCOOH. When polymers **CPIZ-B** and **CPIZ-T** were excited at 360 nm in pure HCOOH, the maximum steady-state emission peaks of **CPIZ-B** and **CPIZ-T** are local at 405 nm and 428 nm, respectively. The emission peaks are red-shifted when the conjugated length is extended. While we did not detect the emission when **CPIZ-B** and **CPIZ-T** were excited at their maximum absorption peaks, indicating that this intramolecular charge transfer state is a non-radiative relaxation path. The excitation spectra of **CPIZ-B** and

CPIZ-T confirm that the photoluminescence originates from the high energy region. This means both **CPIZ-B** and **CPIZ-T** retain the localized emission peaks observed in the fluorene moiety.[S5] These emissions could be attributed to the twisted structures of the **CPIZ-B** and **CPIZ-T**, leading to twisted intramolecular charge transfer (TICT),[S6] resulting in the fluorescence from the high energy band through relaxation of the locally excited state and non-radiative relaxation channels in the low energy band. Time-resolved photoluminescence was carried out (exciting the samples at ~263 nm) to understand the dynamics of the emission, streak images are shown in the Figure S10. **CPIZ-B** showed a longer lifetime, with emission decay exceeding 2000 ps which was the maximum measurable lifetime of the streak camera unit, while **CPIZ-T** showed bimodal-exponential emission decay with lifetimes of 146 ps and 969 ps. The longer life time of **CPIZ-B** is because of higher twisted structures of the **CPIZ-B** than that of **CPIZ-T** which lead to less effective intramolecular charge transfer in **CPIZ-B**. **CPIZ-T** has a better planar structure compared to the **CPIZ-B** due to having smaller torsional angles between the thiphene moiety and tritylium resulting in higher effective charge transfer in **CPIZ-T** and reduced lifetime.

It is well-known that for doped conjugated polymers, polarons are extremely efficient exciton quenchers and even in low concentration, photoluminescene is effectively quenched.[S5,S7,S8] Thus, the presence of photoluminescence in **CPIZ-B** and **CPIZ-T** proves that our CPIs-polymers are intrinsic polymers rather than doped polymers.

2.6 Film Morphology

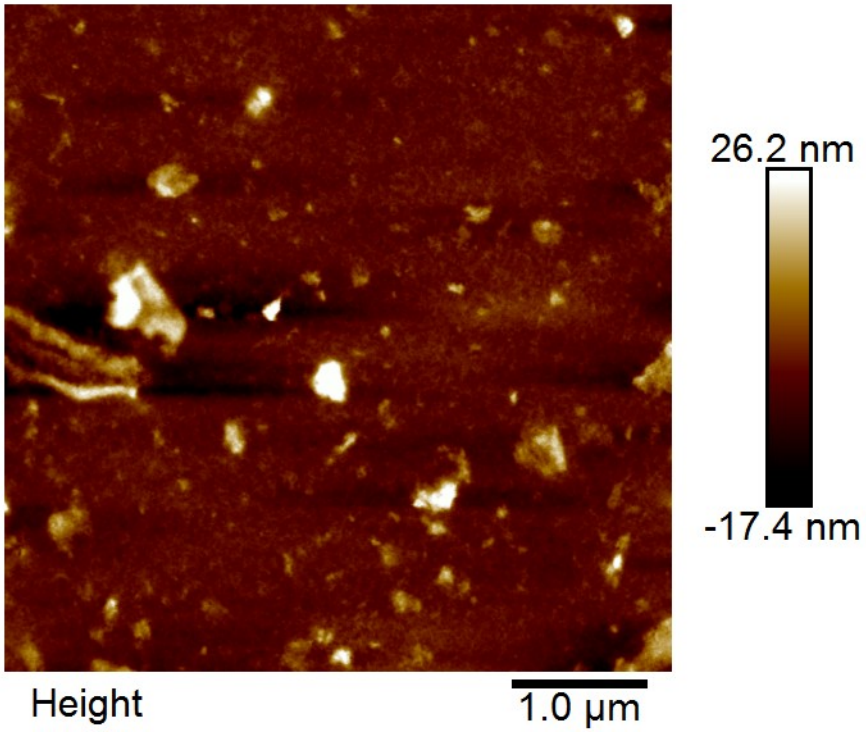

Figure S11: Surface topographic AFM image of **CPIZ-B** bare glass surface (25 μm^2) when cast from 10 mg mL^{-1} in pure HCOOH. The RMS roughness is 4.68 nm.

2.7 EQE data of bi-layer solar cells

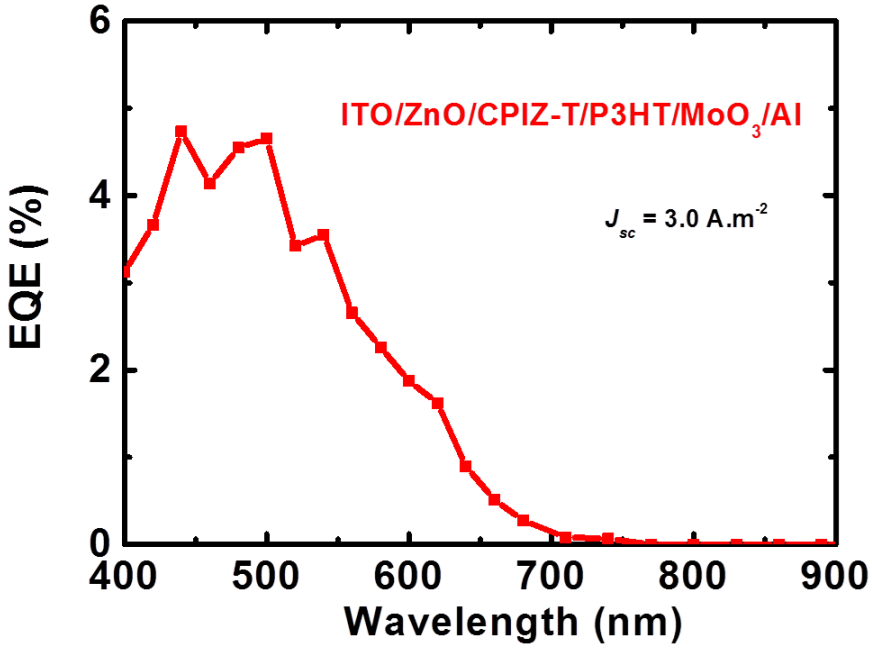

Figure S12: EQE spectra of the all polymer bi-layer solar cells devices based on **CPIZ-T** and P3HT, and **CPIZ-T** spun-cast from pure (HCOOH).

3 DFT calculations

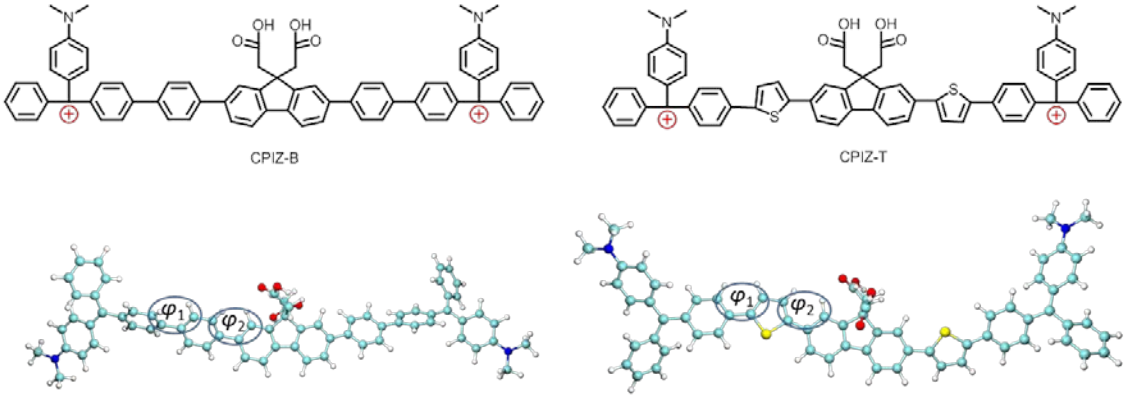

Figure S13: DFT-optimized geometries of the repeating units of **CPIZ-B** and **CPIZ-T**, the dihedral angles between the planes of π-system bridge and fluorene moiety or trityllium moiety and the regions of steric repulsion torsion are indicated by the circles.

4 SCLC measurement

Figure S14 shows trace-retrace J-V curves of the two CPIs; CPIZ-B shows no hysteresis when cast from HCOOH with or without H_2O, while CPIZ-T shows only a very slight hysteresis between voltages of 0 to 1.5 V. These plots clearly show that the influence of any residual free ions on the total conductivity is negligible

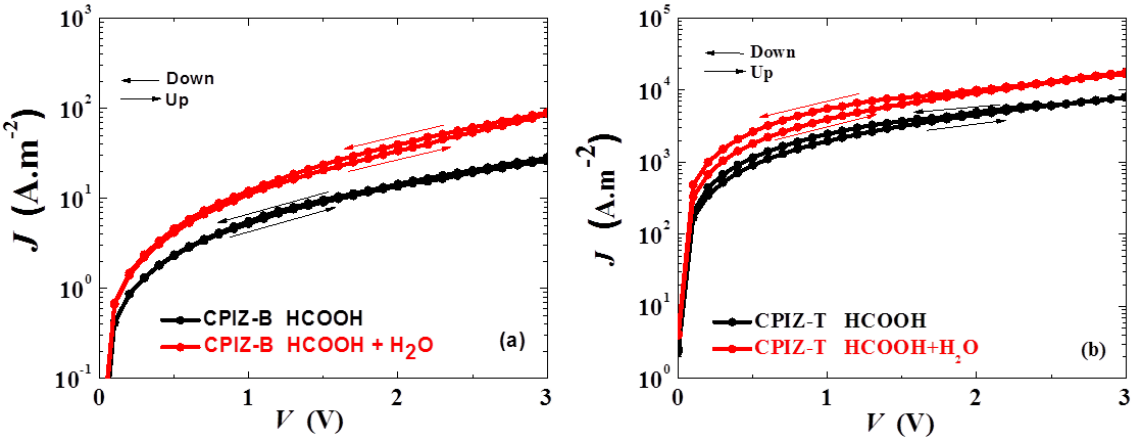

Figure S14: Current-voltage characteristics with sweep up/down of electron-only devices for thin films of a) **CPIZ-B** cast from pure HCOOH and from 80:20 v % HCOOH:H_2O; and b) **CPIZ-T** cast from pure HCOOH and from 80:20 v% HCOOH:H_2O.

5 Impedance device

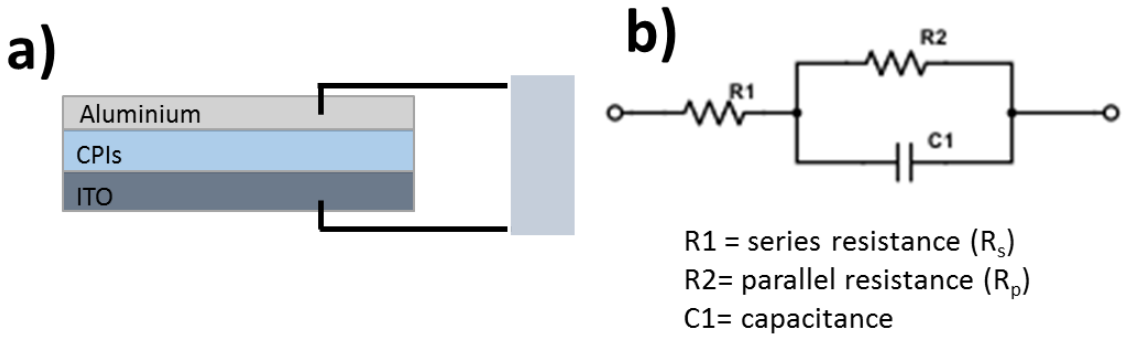

Figure S15: a) Device architecture for the impedance measurement for thin films of **CPIZ-T** cast from pure HCOOH. b) Equivalent circuit used for fitting impedance data. R_1 represents the series resistance due to contact resistance and probe effects. The parallel resistance R_2 is needed to account for the finite resistance of real materials, and C_1 represents an ideal capacitor.

6 Impedance data

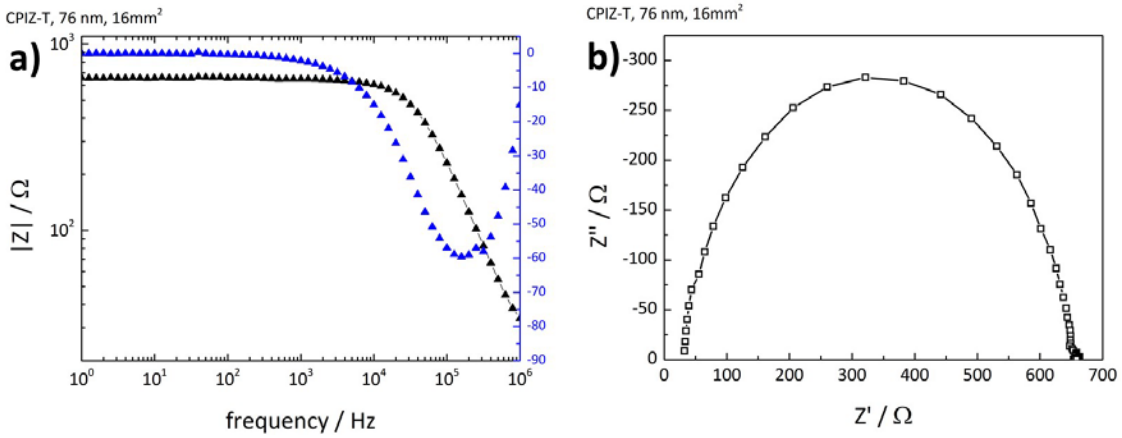

Figure S16: a) Bode plots and b) Nyquist impedance plot for **CPIZ-T**. The measured data of the magnitude (|Z|, black triangles) and the phase (blue triangles) are plotted against the frequency, the Nyquist diagram of the device is plotted showing the behavior of a real capacitor.

References

(S1) Qin, C.; Wu, X.; Tong, H.; Wang, L. High solubility and photoluminescence quantum yield water-soluble polyfluorenes with dendronized amino acid side chains: synthesis, photophysical, and metal ion sensing properties. *Journal of Materials Chemistry* **2010**, *20*, 7957–7964.

(S2) Chen, X.; Chang, G. Synthesis and Photosensitive Properties of Poly (aryl imino) Containing Azobenzene Group (PAI-A). *Chinese Journal of Chemistry* **2009**, *27*, 2093–2096.

(S3) Bartholome, D.; Klemm, E. Novel polyarylene-triarylmethane dye copolymers. *Macromolecules* **2006**, *39*, 5646–5651.

(S4) Mai, C.-k.; Arai, T.; Liu, X.; Fronk, S. L.; Su, G. M.; Segalman, R. A.; Chabinyc, L.; Bazan, G. C. Electrical properties of doped conjugated polyelectrolytes with modulated density of the ionic functionalities †. *Chemical Communications* **2015**, 1–4.

(S5) Lee, B. H.; Lee, J.-h.; Jeong, S. Y.; Park, S. B.; Lee, S. H.; Lee, K. Broad Work-Function Tunability of p-Type Conjugated Polyelectrolytes for Effi cient Organic Solar Cells. *Adv. Energy Mater* **2015**, *5*, 1401653.

(S6) Sasaki, S.; Drummen, G. P.; Konishi, G. I. Recent advances in twisted intramolecular charge transfer (TICT) fluorescence and related phenomena in materials chemistry. *Journal of Materials Chemistry C* **2016**, *4*, 2731–2743.

(S7) Jacobs, I. E.; Wang, F.; Hafezi, N.; Medina-Plaza, C.; Harrelson, T. F.; Li, J.; Augustine, M. P.; Mascal, M.; Moulé, A. J. Quantitative Dedoping of Conductive Polymers. *Chemistry of Materials* **2017**, *29*, 832–841.

(S8) Lee, J.-h.; Lee, B. H.; Jeong, S. Y.; Park, S. B.; Kim, G.; Lee, S. H.; Lee, K. Radical

Cation – Anion Coupling-Induced Work Function Tunability in Anionic Conjugated Polyelectrolytes. *Adv. Energy Mater* **2015**, *5*, 1501292.